ALMA MATER STUDIORUM
UNIVERSITÀ DI BOLOGNA

ARCHIVIO ISTITUZIONALE
DELLA RICERCA

Alma Mater Studiorum Università di Bologna
Archivio istituzionale della ricerca

Planar class A Bézier curves: The case of real eigenvalues

This is the final peer-reviewed author's accepted manuscript (postprint) of the following publication:

Published Version:
Romani L., Viscardi A. (2021). Planar class A Bézier curves: The case of real eigenvalues. COMPUTER AIDED GEOMETRIC DESIGN, 89, 1-14 [10.1016/j.cagd.2021.102021].

Availability:
This version is available at: https://hdl.handle.net/11585/831309 since: 2021-09-06

Published:
DOI: http://doi.org/10.1016/j.cagd.2021.102021

Terms of use:

Some rights reserved. The terms and conditions for the reuse of this version of the manuscript are specified in the publishing policy. For all terms of use and more information see the publisher's website.

This item was downloaded from IRIS Università di Bologna (https://cris.unibo.it/).
When citing, please refer to the published version.

(Article begins on next page)

12 October 2024

This is the final peer-reviewed accepted manuscript of:

Lucia Romani, Alberto Viscardi, Planar class A Bézier curves: The case of real eigenvalues, Computer Aided Geometric Design 89, 102021 (2021)

The final published version is available online at ***https://dx.doi.org/10.1016/j.cagd.2021.102021***

Rights / License:

The terms and conditions for the reuse of this version of the manuscript are specified in the publishing policy. For all terms of use and more information see the publisher's website.

This item was downloaded from IRIS Università di Bologna (https://cris.unibo.it/)

When citing, please refer to the published version.

Planar Class A Bézier Curves: The Case of Real Eigenvalues

Lucia Romani[a], Alberto Viscardi[a,]

[a] *Dipartimento di Matematica, Alma Mater Studiorum Università di Bologna, Piazza di Porta San Donato 5, 40126 Bologna, Italy*

Abstract

We consider planar, special Bézier curves, i.e., polynomial Bézier curves in the plane whose control polygon is fully identified by the first edge and a 2×2 matrix $\mathbf{M}$. We focus on the case where $\mathbf{M}$ has two real eigenvalues and we formulate, in terms of the Schur form of $\mathbf{M}$, necessary and sufficient conditions for a regular, planar special Bézier curve to be a class A curve, i.e., a curve with monotone curvature, for any degree and any choice of the first edge. The result is simple in its formulation and can thus be easily used for both designing class A curves and analyzing given special Bézier curves.

Keywords: planar curves, Bézier curves, class A curves, monotone curvature

1. Introduction

Bézier curves are polynomial curves described by a sequence of control points related to the Bernstein basis functions, and provide an intuitive design tool in many industrial applications. Special Bézier curves form a subfamily of Bézier curves for which, given an initial control point $\mathbf{p}_0$ and an initial control vector $\mathbf{v} \neq \mathbf{0}$, all the successive control points $\mathbf{p}_k$ are obtained by further applications of a matrix $\mathbf{M}$, i.e.

$$\mathbf{p}_k \;=\; \mathbf{p}_{k-1} \;+\; \mathbf{M}^{k-1}\,\mathbf{v} \;=\; \mathbf{p}_0 \;+\; \sum_{j=0}^{k-1} \mathbf{M}^j\,\mathbf{v}, \qquad k = 1, \ldots, n,$$

where $n \in \mathbb{N}$ is the degree of the Bézier curve. In a nutshell, the control polygon of a special Bézier curve has control legs described by iterative applications of the matrix $\mathbf{M}$ to the vector $\mathbf{v}$. Having a more rigid structure than generic Bézier curves could sound like a drawback from a design perspective, but it actually allows for a better understanding of some geometric properties of the curves.

In this work we assume the representative matrix $\mathbf{M}$ to have real eigenvalues and provide necessary and sufficient conditions for the planar special Bézier curves associated with $\mathbf{M}$ to be of class A, i.e. to have monotone curvature, for every degree n and every choice of the initial control vector $\mathbf{v} \neq \mathbf{0}$. Parametric curves with monotone curvature are considered of interest in industrial design and styling (see, e.g., Cantón et al. (2021); Sapidis and Frey (1992); Wang et al. (2019, 2004)) since they allow to meet the aesthetic requirements needed to achieve the highest grade of shape quality. The ability to construct "fair curves" is what brought Farin (2006) to introduce class A curves. These were meant to be a generalization of the so-called "typical curves", studied in Mineur et al. (1998) and further investigated in Tong and Chen (2021), to obtain a subclass of special Bézier curves fulfilling specific geometrical conditions on the control polygon. Such conditions are encoded in a special choice of the representative matrix $\mathbf{M}$, which is the product of a rotation matrix and a dilation factor. Such a structure of $\mathbf{M}$ was also assumed in Yoshida et al. (2008), where a method for interactively controlling a segment of a class A Bézier curve was presented. Differently, in Farin (2006), the author takes into account special Bézier curves with general representative matrices

*Corresponding author
Email addresses: `lucia.romani@unibo.it` (Lucia Romani), `alberto.viscardi@unibo.it` (Alberto Viscardi)

and searches for conditions involving their singular values that can lead to class A curves. The sufficient conditions for the matrix $\mathbf{M}$ provided in Farin (2006) were successively proved to be incomplete and revised in (Cao and Wang (2008); Wang and Zhao (2018)). However, the sufficient conditions proposed in Cao and Wang (2008) deal with symmetric representative matrices only. The goal of our research is to improve previous results in Cao and Wang (2008); Farin (2006); Wang and Zhao (2018), in order to have a complete characterization of class A representative matrices with real eigenvalues in the planar case.

In contrast to Cantón et al. (2021), where conditions entwining the representative matrix $\mathbf{M}$, the initial control vector $\mathbf{v}$ and the degree n are given to obtain a class A curve, in this work we identify all possible 2×2 matrices with real eigenvalues that lead to planar class A curves for every choice of $\mathbf{v}$ and n. Our approach is justified by the fact that, in this way, two important parameters - the degree of the curve and the initial control vector - are kept free and, moreover, invariance under rotations, translations and dilations is ensured. To reach our goal, besides following Farin's idea of subdividing a special Bézier curve (see Farin (2006)), we exploit invariance under orthogonal transformations and thus we only need to consider 2×2 matrices of the form

$$\mathbf{M}_R \;:=\; \begin{bmatrix} \lambda_0 & c \\ 0 & \lambda_1 \end{bmatrix}, \; \begin{bmatrix} \lambda_0 \\ \lambda_1 \\ c \end{bmatrix} \in \mathbb{R}^3 \setminus \{\mathbf{0}\}. \tag{1}$$

The rest of the paper is structured as follows. In Section 2 we provide a brief review of special Bézier curves. In particular, we recall some convenient representations for the first and the second derivative of a special Bézier curve. These representations are then used in Section 3 to provide the characterization of class A representative matrices with real eigenvalues, see Theorem 3.2. While the proof of Theorem 3.2 is rather technical, its statement is simple (a graphical visualization is available in Figure 1) and can be used as a tool to both design new class A curves and analyze given special Bézier curves. Indeed, we are able to give information about the position of the control points of such curves and to provide an easy-to-use construction method that takes as input the properties of the curve at one endpoint. An example about the application of such a constructive procedure concludes the discussion.

2. Planar special Bézier curves and their key properties

Definition 2.1. A degree-n ($n \in \mathbb{N}$) planar Bézier curve

$$\gamma \;:\; [0,1] \longrightarrow \mathbb{R}^2, \qquad t \longmapsto \sum_{k=0}^{n} \mathbf{p}_k \, B_{n,k}(t),$$

is a *special Bézier curve* if the control points $\mathbf{p}_k \in \mathbb{R}^2$, $k = 0, \ldots, n$ to be associated with the Bernstein basis

$$B_{n,k}(t) \;=\; \binom{n}{k} t^k \, (1-t)^{n-k}, \qquad k = 0, \ldots, n$$

are such that

$$\mathbf{p}_k \;=\; \mathbf{p}_0 \;+\; \sum_{j=0}^{k-1} \mathbf{M}^j \, \mathbf{v}, \qquad \forall k = 1, \ldots, n, \tag{2}$$

for some $\mathbf{M} \in \mathbb{R}^{2\times 2}$ and $\mathbf{v} \in \mathbb{R}^2 \setminus \{\mathbf{0}\}$. The matrix $\mathbf{M}$ is called the *representative matrix* of the special Bézier curve γ. The vector $\mathbf{v}$ is called the *initial control vector* of γ.

We now recall some well-known and easy-to-prove facts about special Bézier curves and their derivatives.

Proposition 2.1. *For any choice of* $\mathbf{p}_0 \in \mathbb{R}^2$, $\mathbf{M} \in \mathbb{R}^{2\times 2}$ *and* $\mathbf{v} \in \mathbb{R}^2 \setminus \{\mathbf{0}\}$, *a degree-n special Bézier curve and its first and second order derivative can be written as*

$$\gamma(t) \;=\; \mathbf{p}_0 \;+\; \sum_{k=1}^{n} \left(\sum_{j=0}^{k-1} \mathbf{M}^j \, \mathbf{v} \right) B_{n,k}(t), \tag{3}$$

$$\gamma'(t) \;=\; n\;[\,(1-t)\mathbf{I} \;+\; t\mathbf{M}\,]^{n-1}\;\mathbf{v}, \tag{4}$$

and

$$\gamma''(t) \;=\; n\,(n-1)\;[\,(1-t)\mathbf{I} \;+\; t\mathbf{M}\,]^{n-2}\;(\mathbf{M}-\mathbf{I})\,\mathbf{v}, \tag{5}$$

respectively. Moreover, γ is regular (i.e., $\|\gamma'(t)\| > 0, \forall\, t \in [0,1]$) if and only if the spectrum of $\mathbf{M}$, $\mathrm{spec}(\mathbf{M})$, *satisfies*

$$\mathrm{spec}(\mathbf{M}) \cap (-\infty, 0] \;=\; \emptyset. \tag{6}$$

The proof of Proposition 2.1 is omitted since it follows straightforwardly recalling Definition 2.1 and the formula for the first and second order derivative of Bernstein polynomials.

Remark 2.2. As for (3), $\gamma(0) = \mathbf{p}_0$ and so $\mathbf{p}_0$ is the first endpoint of the special Bézier curve γ, while $\mathbf{v}$ specifies the tangent direction at the same location since, in view of (4), $\gamma'(0) = n\mathbf{v}$. It is also worth noting that, in light of (4) and (5), $\mathbf{p}_0$ does not affect in any way γ' and γ''. Moreover, $\mathbf{v}$ acts in both derivatives only as a multiplicative factor and for what follows we can always consider $\|\mathbf{v}\| = 1$ without loss of generality.

We conclude this section with a preliminary result providing the value attained by the curvature

$$\kappa(t) \;=\; \frac{\sqrt{\|\gamma'(t)\|^2\;\|\gamma''(t)\|^2 - \left(\gamma'(t)^T\gamma''(t)\right)^2}}{\|\gamma'(t)\|^3} \tag{7}$$

of a regular, planar, special Bézier curve γ at the endpoints $t = 0$ and $t = 1$.

Proposition 2.3. *Let γ be a regular, planar special Bézier curve of degree n with representative matrix $\mathbf{M} \in \mathbb{R}^{2\times 2}$ and unit initial control vector $\mathbf{v} \in \mathbb{R}^2$, and let*

$$F(\mathbf{M},\mathbf{v}) \;:=\; 4\|(\mathbf{M} \;-\; \mathbf{I})\mathbf{v}\|^2 \;-\; \left(\,\|\mathbf{M}\mathbf{v}\|^2 \;-\; \|(\mathbf{M} \;-\; \mathbf{I})\mathbf{v}\|^2 \;-\; 1\,\right)^2. \tag{8}$$

Then,

$$\kappa(0) \;=\; \frac{n-1}{2n}\,\sqrt{F(\mathbf{M},\mathbf{v})}, \tag{9}$$

and

$$\kappa(1) \;=\; \frac{n-1}{2n}\,\frac{\|\mathbf{M}^{n-2}\mathbf{v}\|^2}{\|\mathbf{M}^{n-1}\mathbf{v}\|^3}\,\sqrt{F(\mathbf{M},\mathbf{w})} \qquad \textit{with} \qquad \mathbf{w} = \mathbf{M}^{n-2}\mathbf{v}/\|\mathbf{M}^{n-2}\mathbf{v}\|. \tag{10}$$

Proof. We begin manipulating (7) to get

$$4\,(\,\kappa(t)\,)^2 \;=\; \frac{4\,\|\gamma'(t)\|^2\,\|\gamma''(t)\|^2 \;-\; \left(\,2\,\gamma'(t)^T\,\gamma''(t)\,\right)^2}{\|\gamma'(t)\|^6}. \tag{11}$$

Evaluating (4) and (5) at $t = 0$ and $t = 1$, we respectively obtain

$$\gamma'(0) \;=\; n\mathbf{v}, \quad \gamma''(0) \;=\; n(n-1)(\mathbf{M} \;-\; \mathbf{I})\mathbf{v}, \quad \gamma'(1) \;=\; n\mathbf{M}^{n-1}\mathbf{v}, \quad \gamma''(1) \;=\; n(n-1)\mathbf{M}^{n-2}(\mathbf{M} \;-\; \mathbf{I})\mathbf{v}.$$

Combining (11) with these equalities, recalling that $\mathbf{v}^T\mathbf{M}^T\mathbf{v} = \mathbf{v}^T\mathbf{M}\mathbf{v}$, that

$$\|(\mathbf{M} \;-\; \mathbf{I})\mathbf{v}\|^2 \;=\; \|\mathbf{M}\mathbf{v}\|^2 \;-\; 2\mathbf{v}^T\mathbf{M}\mathbf{v} \;+\; \|\mathbf{v}\|^2 \quad\longrightarrow\quad 2\mathbf{v}^T\mathbf{M}\mathbf{v} \;-\; \|\mathbf{v}\|^2 \;=\; \|\mathbf{M}\mathbf{v}\|^2 \;-\; \|(\mathbf{M} \;-\; \mathbf{I})\mathbf{v}\|^2,$$

and $\|\mathbf{v}\| = 1$, we get

$$\begin{aligned} 4\left(\frac{n}{n-1}\right)^2(\,\kappa(0)\,)^2 \;&=\; \frac{4\,\|\mathbf{v}\|^2\,\|(\mathbf{M} \;-\; \mathbf{I})\mathbf{v}\|^2 \;-\; \left(\,2\mathbf{v}^T\mathbf{M}\mathbf{v} \;-\; 2\|\mathbf{v}\|^2\,\right)^2}{\|\mathbf{v}\|^6} \\ &=\; 4\|(\mathbf{M}-\mathbf{I})\mathbf{v}\|^2 \;-\; \left(\,\|\mathbf{M}\mathbf{v}\|^2 \;-\; \|(\mathbf{M} \;-\; \mathbf{I})\mathbf{v}\|^2 \;-\; 1\,\right)^2 \;=\; F(\mathbf{M},\mathbf{v}), \end{aligned}$$

from which $F(\mathbf{M},\mathbf{v}) \;\geq\; 0$ and (9) follows. Similarly one gets (10). □

3. Class A property for representative matrices with real eigenvalues

Definition 3.1. A planar parametric curve $\gamma : [0,1] \to \mathbb{R}^2$ is a *class A curve* if it is two times differentiable, regular and its curvature is a monotonic function of $t \in [0,1]$.

Let γ be the special Bézier curve of degree n defined by the initial control point $\mathbf{p}_0$, the representative matrix $\mathbf{M}$ with real eigenvalues and the initial control vector $\mathbf{v}$. Since, in order to be a class A curve, γ has to be regular, due to (6) we only consider $\mathbf{M}$ with strictly positive real eigenvalues.

Now, exploiting the formulation of γ'' in (5), we show that the class A property is invariant under orthogonal transformations. This justifies the need to study $\mathbf{M}$ only in its Schur form (1).

Proposition 3.1. *Let $\mathbf{M} \in \mathbb{R}^{2\times 2}$. The following statements are equivalent:*

(i) the curve $\gamma(t)$ in (3) is a class A curve for every $n \in \mathbb{N}$, $\mathbf{p}_0 \in \mathbb{R}^2$, $\mathbf{v} \in \mathbb{R}^2 \setminus \{\mathbf{0}\}$;

(ii) the curve

$$\zeta(t) \;=\; \mathbf{q}_0 \;+\; \sum_{k=1}^{n} \left(\sum_{j=0}^{k-1} (\mathbf{Q}^T\mathbf{M}\mathbf{Q})^j \, \mathbf{w} \right) B_{n,k}(t)$$

is a class A curve for every $n \in \mathbb{N}$, $\mathbf{q}_0 \in \mathbb{R}^2$, $\mathbf{w} \in \mathbb{R}^2 \setminus \{\mathbf{0}\}$ and $\mathbf{Q} \in \mathbb{R}^{2\times 2}$ orthogonal.

Proof. $(ii) \Rightarrow (i)$: It is enough to choose $\mathbf{q}_0 = \mathbf{p}_0$, $\mathbf{w} = \mathbf{v}$ and $\mathbf{Q} = \mathbf{I}$;
$(i) \Rightarrow (ii)$: Observe that, since $\mathbf{Q}$ is orthogonal, $(\mathbf{Q}^T\mathbf{M}\mathbf{Q})^j = \mathbf{Q}^T\,\mathbf{M}^j\,\mathbf{Q}$. Choose $\mathbf{p}_0 = \mathbf{Q}\mathbf{q}_0$ and $\mathbf{v} = \mathbf{Q}\mathbf{w}$. Then, $\zeta(t) - \mathbf{Q}^T\gamma(t) \equiv 0$. In particular, $\zeta(t)$ and $\mathbf{Q}^T\gamma(t)$ have the same curvature. Since $\mathbf{Q}$ is orthogonal, we also have that $\mathbf{Q}^T\gamma(t)$ and $\gamma(t)$ have the same curvature. Therefore, since $\gamma(t)$ is a class A curve, also $\mathbf{Q}^T\gamma(t)$ and $\zeta(t)$ are class A curves. □

Now we are ready to show the main result of this paper. The strategy adopted follows Farin's idea of subdividing a special Bézier curve (see Farin (2006)). In particular, we recall that, subdividing a special Bézier curve at $r \in (0,1)$, leads to two special Bézier curves $\gamma_{[0,r]}$ and $\gamma_{[r,1]}$ described respectively by the well-defined representative matrices

$$\mathbf{M}_{[0,r]} \;:=\; (1-r)\mathbf{I} \;+\; r\mathbf{M} \quad \text{and} \quad \mathbf{M}_{[r,1]} \;:=\; \mathbf{M}\,\mathbf{M}_{[0,r]}^{-1}. \tag{12}$$

Since regularity and monotonicity of the curvature are trivially invariant under subdivisions, we search for properties of $\mathbf{M}$ that imply $\kappa(0) \geq \kappa(1)$ (or $\kappa(0) \leq \kappa(1)$) and are inherited by $\mathbf{M}_{[0,r]}$ and $\mathbf{M}_{[r,1]}$, for all $r \in (0,1)$.

Theorem 3.2. *Let $\mathbf{M} \equiv \mathbf{M}_R$ as in (1). The special Bézier curve with representative matrix $\mathbf{M}$ is a class A curve for every degree and every initial control vector if and only if*

$$\begin{cases} \lambda_0 \geq 1, \\[2ex] \dfrac{\lambda_0+1}{2} \leq \lambda_1 \leq 2\lambda_0 - 1, \\[2ex] c^2 \leq \dfrac{4}{9}(2\lambda_0 - \lambda_1 - 1)(2\lambda_1 - \lambda_0 - 1), \end{cases} \tag{13}$$

or

$$\begin{cases} 0 < \lambda_0 < 1, \\[2ex] \dfrac{\lambda_0}{2-\lambda_0} \leq \lambda_1 \leq \dfrac{2\lambda_0}{\lambda_0+1}, \\[2ex] c^2 \leq \dfrac{4}{9}(2\lambda_0 - \lambda_1 - \lambda_0\lambda_1)(2\lambda_1 - \lambda_0 - \lambda_0\lambda_1). \end{cases} \tag{14}$$

Moreover, the curvature is non-increasing if $\lambda_0 \geq 1$ and non-decreasing if $\lambda_0 \in (0,1)$.

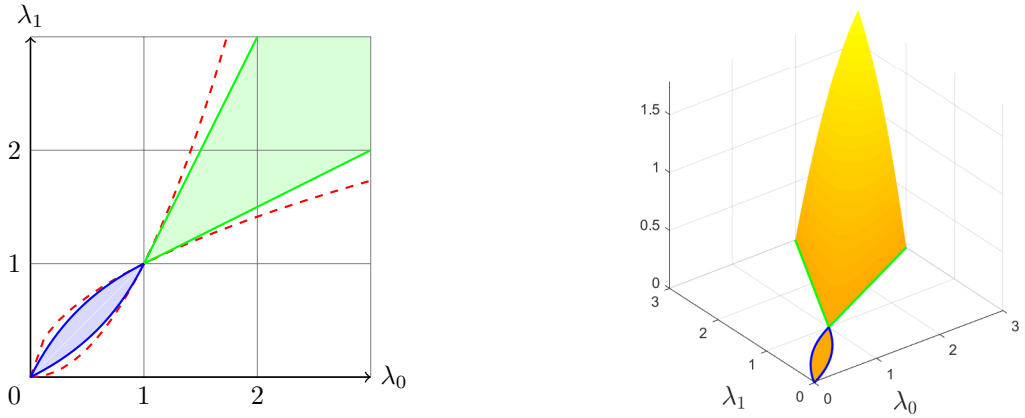

Figure 1: Graphical interpretation of Theorem 3.2. Left: in red the lines $\lambda_1 = \lambda_0^2$ and $\lambda_1 = \sqrt{\lambda_0}$; in green the area $\lambda_0 \geq 1 \ \wedge \ (\lambda_0 + 1)/2 \leq \lambda_1 \leq 2\lambda_0 - 1$ leading to class A curves with non-increasing curvature; in blue the area $0 < \lambda_0 < 1 \ \wedge \ \lambda_0/(2-\lambda_0) \leq \lambda_1 \leq 2\lambda_0/(\lambda_0+1)$ leading to class A curves with non-decreasing curvature. Right: the surface described by the upper bound for c^2 in (13). (For interpretation of the colors in the figure legend, the reader is referred to the web version of this article.)

A graphical interpretation of the regions described by (13) and (14) is shown in Figure 1. The proof of Theorem 3.2 is, on one hand, the core of this work. However, on the other hand, it is rather technical and it does not give direct insights about the construction and the properties of class A curves generated by matrices with Schur form satisfying (13) or (14). Thus, we prefer to postpone it to Appendix A, while we here proceed by extracting all those information about the control polygon of these curves that are not self-apparent.

Before doing that, we would like to show with an example the possibilities opened up by Theorem 3.2 with respect to Cao and Wang (2008). There, the considered matrices are always symmetric, which means that c is always set to 0. However, different values of c, within the ranges described by (13) and (14), yield different behaviours of the resulting class A curve, as illustrated in Example 3.1.

Example 3.1. Let $n = 7$, $\mathbf{p}_0 = \mathbf{0}$ and $\mathbf{v} = [1, 0]^T$. We consider the set of matrices

$$\left\{ \begin{bmatrix} \cos(\pi/3) & \sin(\pi/3) \\ -\sin(\pi/3) & \cos(\pi/3) \end{bmatrix} \begin{bmatrix} 4 & c \\ 0 & 3 \end{bmatrix} \begin{bmatrix} \cos(\pi/3) & -\sin(\pi/3) \\ \sin(\pi/3) & \cos(\pi/3) \end{bmatrix} : c \in \left\{ -\frac{4}{3}, -\frac{2}{3}, 0, \frac{2}{3}, \frac{4}{3} \right\} \right\}$$

satisfying (13) and the set of matrices

$$\left\{ \begin{bmatrix} \cos(\pi/3) & \sin(\pi/3) \\ -\sin(\pi/3) & \cos(\pi/3) \end{bmatrix} \begin{bmatrix} \frac{1}{3} & c \\ 0 & \frac{1}{4} \end{bmatrix} \begin{bmatrix} \cos(\pi/3) & -\sin(\pi/3) \\ \sin(\pi/3) & \cos(\pi/3) \end{bmatrix} : c \in \left\{ -\frac{1}{9}, -\frac{1}{18}, 0, \frac{1}{18}, \frac{1}{9} \right\} \right\}$$

satisfying (14). The corresponding class A special Bézier curves defined as in (3) are depicted in Figure 2 along with their curvatures. There, the dotted lines represent the cases with $c = 0$ and it it easy to see how changing c modifies the shape and the behaviour of the curvature of the resulting curves.

Now, with the precise bounds given in Theorem 3.2 one can prove the following geometric facts that lead to an easy-to-use constructive method for planar class A curves with prescribed features at one of the endpoints. For simplicity we consider only the first endpoint, but the same arguments can be used for the other endpoint, since a class A special Bézier curve travelled backward is still a class A special Bézier curve, having as the representative matrix the inverse of the starting representative matrix.

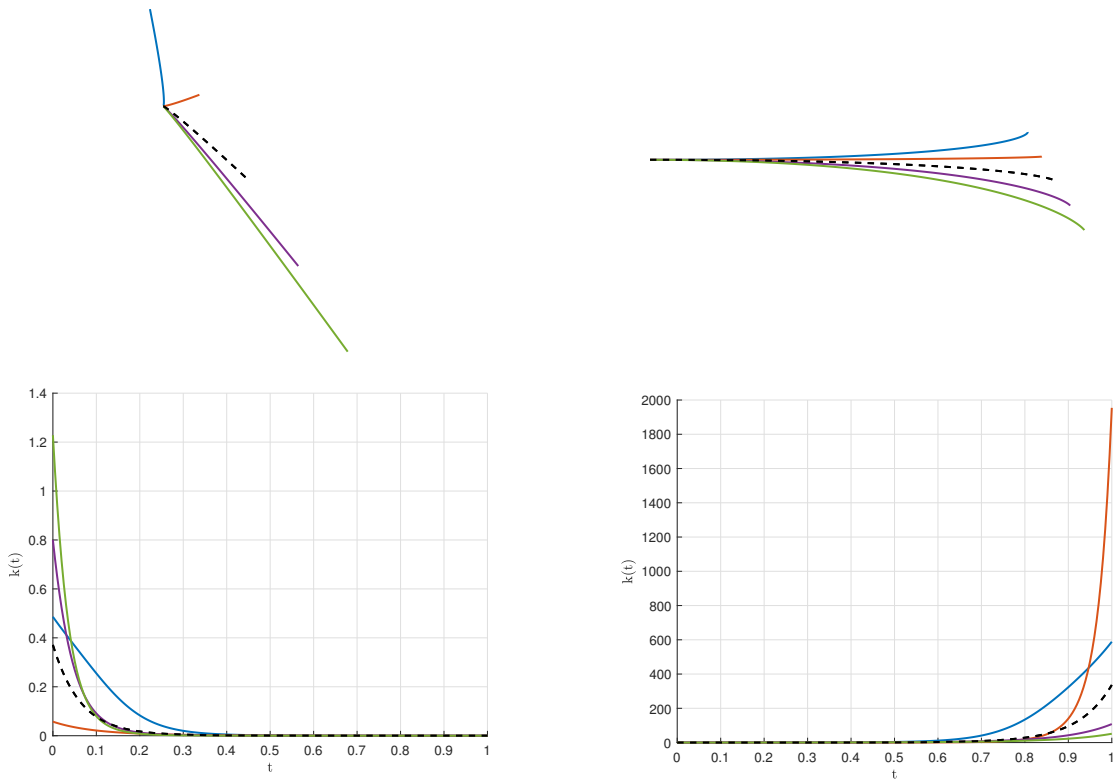

Figure 2: The class A special Bézier curves described in Example 3.1 and their associated curvature plots: on the left hand side, the ones satisfying conditions (13); on the right hand side, the ones satisfying conditions (14). The dotted lines correspond to the cases with $c = 0$, already investigated in Cao and Wang (2008).

Corollary 3.3. *Let $\rho > 0$, $\theta \in [0, 2\pi)$ and $\mathbf{v} = \rho[\cos(\theta), \sin(\theta)]^T$ and define the subsets of $\mathbb{R}^2$*

$$\mathcal{P}_{\geq 1}(\mathbf{v}) \;:=\; \{\, \mathbf{M}\mathbf{v} + \mathbf{v} \;:\; \mathbf{M} \equiv \mathbf{M}_R \text{ satisfying (13)} \,\}$$

and

$$\mathcal{P}_{<1}(\mathbf{v}) \;:=\; \{\, \mathbf{M}\mathbf{v} + \mathbf{v} \;:\; \mathbf{M} \equiv \mathbf{M}_R \text{ satisfying (14)} \,\}.$$

Then

$$\mathcal{P}_{\geq 1}(\mathbf{v}) \;=\; \left\{ \begin{bmatrix} \cos(\theta) & -\sin(\theta) \\ \sin(\theta) & \cos(\theta) \end{bmatrix} \mathbf{w} \;:\; \mathbf{w} \in \mathcal{P}_{\geq 1}\left(\begin{bmatrix} \rho \\ 0 \end{bmatrix} \right) \right\}$$

and

$$\mathcal{P}_{<1}(\mathbf{v}) \;=\; \left\{ \begin{bmatrix} \cos(\theta) & -\sin(\theta) \\ \sin(\theta) & \cos(\theta) \end{bmatrix} \mathbf{w} \;:\; \mathbf{w} \in \mathcal{P}_{<1}\left(\begin{bmatrix} \rho \\ 0 \end{bmatrix} \right) \right\},$$

where

$$\mathcal{P}_{\geq 1}\left(\begin{bmatrix} \rho \\ 0 \end{bmatrix} \right) \;:=\; \left\{ \begin{bmatrix} x \\ y \end{bmatrix} \in \mathbb{R}^2 \;:\; x \geq 2\rho \;\wedge\; -\frac{3}{4}(x - 2\rho) \leq y \leq \frac{3}{4}(x - 2\rho) \right\} \tag{15}$$

and

$$\begin{aligned} \mathcal{P}_{<1}\left(\begin{bmatrix} \rho \\ 0 \end{bmatrix} \right) \;:=\; \Bigg\{ \begin{bmatrix} x \\ y \end{bmatrix} \in \mathbb{R}^2 \;:\; \rho < x < 2\rho \;\wedge \\ \frac{2}{3}\rho - \sqrt{\frac{25}{36}\rho^2 - \left(x - \frac{3}{2}\rho\right)^2} \leq y \leq -\frac{2}{3}\rho + \sqrt{\frac{25}{36}\rho^2 - \left(x - \frac{3}{2}\rho\right)^2} \Bigg\}. \end{aligned} \tag{16}$$

In particular, for every $\mathbf{p} = [x, y]^T \in \mathcal{P}_{\geq 1}(\mathbf{v}) \cup \mathcal{P}_{<1}(\mathbf{v})$*, the matrix*

$$\mathbf{M} \;=\; \begin{bmatrix} \cos(\theta) & -\sin(\theta) \\ \sin(\theta) & \cos(\theta) \end{bmatrix} \begin{bmatrix} \dfrac{\widetilde{x}}{\rho} - 1 & \dfrac{\widetilde{y}}{\rho} + c \\ \dfrac{\widetilde{y}}{\rho} & 2\lambda - \dfrac{\widetilde{x}}{\rho} + 1 \end{bmatrix} \begin{bmatrix} \cos(\theta) & \sin(\theta) \\ -\sin(\theta) & \cos(\theta) \end{bmatrix} \tag{17}$$

where

$$\begin{bmatrix} \widetilde{x} \\ \widetilde{y} \end{bmatrix} \;=\; \begin{bmatrix} \cos(\theta) & \sin(\theta) \\ -\sin(\theta) & \cos(\theta) \end{bmatrix} \mathbf{p},$$

$$\lambda \;=\; \begin{cases} \dfrac{3(\widetilde{x} - \rho) + |\widetilde{y}| \;\pm\; \sqrt{2|\widetilde{y}|(3\widetilde{x} - 6\rho - 4|\widetilde{y}|)}}{3\rho}, & \text{if } \mathbf{p} \in \mathcal{P}_{\geq 1}(\mathbf{v}), \\[2ex] \dfrac{3(\widetilde{x} - \rho) + |\widetilde{y}| \;\pm\; \sqrt{2|\widetilde{y}|(9\rho\widetilde{x} - 6\rho^2 - 3\widetilde{x}^2 - 3\widetilde{y}^2 - 4\rho|\widetilde{y}|)/\rho}}{3\rho \;+\; 2|\widetilde{y}|}, & \text{if } \mathbf{p} \in \mathcal{P}_{<1}(\mathbf{v}), \end{cases} \tag{18}$$

and

$$c \;=\; \begin{cases} -\operatorname{sgn}(\widetilde{y})\dfrac{2}{3}(\lambda - 1), & \text{if } \mathbf{p} \in \mathcal{P}_{\geq 1}(\mathbf{v}), \\[2ex] -\operatorname{sgn}(\widetilde{y})\dfrac{2}{3}\lambda(1 - \lambda), & \text{if } \mathbf{p} \in \mathcal{P}_{<1}(\mathbf{v}), \end{cases} \tag{19}$$

is such that $\mathbf{p} = \mathbf{M}\mathbf{v} + \mathbf{v}$ *and* $\mathbf{M} \equiv \mathbf{M}_R$ *satisfying* (13) *when* $\mathbf{p} \in \mathcal{P}_{\geq 1}(\mathbf{v})$ *or* (14) *when* $\mathbf{p} \in \mathcal{P}_{<1}(\mathbf{v})$*.*

Remark 3.4. The set $\mathcal{P}_{\geq 1}([\rho, 0]^T)$ is a cone with vertex at $[2\rho, 0]^T$ and the set $\mathcal{P}_{<1}([\rho, 0]^T)$ is the intersection of two disks having the same radius $5\rho/6$ and centers $[3\rho/2, \pm 2\rho/3]^T$ respectively, as shown in Figure 3. Note that these two sets have a structure very similar to the ones of Figure 1 left.

Proof of Corollary 3.3. Up to a rotation in $\mathbb{R}^2$, we can consider $\theta = 0$, i.e., $\mathbf{v} = [\rho, 0]^T$, $\rho > 0$, without loss of generality. The proof of (15) and (16) follows from manipulating algebraically (13) and (14), recalling that $\mathbf{M} \equiv \mathbf{M}_R$ if and only if

$$\begin{aligned} \mathbf{M} \;&=\; \begin{bmatrix} \cos(\varphi) & \sin(\varphi) \\ -\sin(\varphi) & \cos(\varphi) \end{bmatrix} \begin{bmatrix} \lambda_0 & c \\ 0 & \lambda_1 \end{bmatrix} \begin{bmatrix} \cos(\varphi) & -\sin(\varphi) \\ \sin(\varphi) & \cos(\varphi) \end{bmatrix} \\ &=\; \begin{bmatrix} -\dfrac{\lambda_1 - \lambda_0}{2}\cos(2\varphi) + \dfrac{c}{2}\sin(2\varphi) + \dfrac{\lambda_0 + \lambda_1}{2} & \dfrac{\lambda_1 - \lambda_0}{2}\sin(2\varphi) + \dfrac{c}{2}\cos(2\varphi) + \dfrac{c}{2} \\ \dfrac{\lambda_1 - \lambda_0}{2}\sin(2\varphi) + \dfrac{c}{2}\cos(2\varphi) - \dfrac{c}{2} & \dfrac{\lambda_1 - \lambda_0}{2}\cos(2\varphi) - \dfrac{c}{2}\sin(2\varphi) + \dfrac{\lambda_0 + \lambda_1}{2} \end{bmatrix}, \end{aligned} \tag{20}$$

for some $\varphi \in [0, 2\pi)$. Consider now $\mathbf{p} = [x, y]^T \in \mathcal{P}_{\geq 1}([\rho, 0]^T)$. Under the assumption $\mathbf{v} = [\rho, 0]^T$, we have $[x, y] \;=\; [\widetilde{x}, \widetilde{y}]$. Condition $\mathbf{p} = \mathbf{M}\mathbf{v} + \mathbf{v}$, along with (20), is equivalent to

$$\begin{bmatrix} x \\ y \end{bmatrix} \;=\; \mathbf{M}\mathbf{v} \;+\; \mathbf{v} \;=\; \rho \begin{bmatrix} -\dfrac{\lambda_1 - \lambda_0}{2}\cos(2\varphi) \;+\; \dfrac{c}{2}\sin(2\varphi) \;+\; \dfrac{\lambda_0 + \lambda_1}{2} + 1 \\ \dfrac{\lambda_1 - \lambda_0}{2}\sin(2\varphi) \;+\; \dfrac{c}{2}\cos(2\varphi) \;-\; \dfrac{c}{2} \end{bmatrix}. \tag{21}$$

In particular, from (21) it is easy to rewrite (20) as

$$\mathbf{M} \;=\; \begin{bmatrix} \dfrac{x}{\rho} - 1 & \dfrac{y}{\rho} + c \\ \dfrac{y}{\rho} & \lambda_0 + \lambda_1 - \dfrac{x}{\rho} + 1 \end{bmatrix} \tag{22}$$

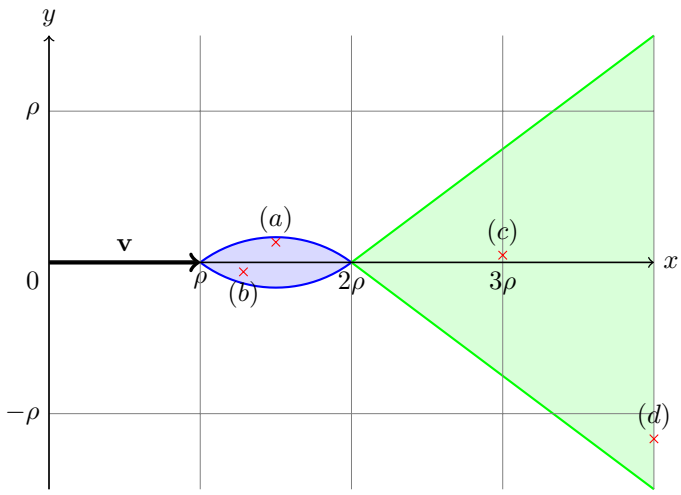

Figure 3: Graphical interpretation of Corollary 3.3. The green and blue areas represent $\mathcal{P}_{\geq 1}(\mathbf{v})$ and $\mathcal{P}_{<1}(\mathbf{v})$, respectively, for $\mathbf{v} = [\rho, 0]^T$, $\rho > 0$. The red crosses (a), (b), (c) and (d) denote the choices of $\mathbf{p}_2$ in Example 3.2. (For interpretation of the colors in the figure legend, the reader is referred to the web version of this article.)

and to prove that

$$\left(\frac{x}{\rho} - \frac{\lambda_0 + \lambda_1 + 2}{2}\right)^2 + \left(\frac{y}{\rho} + \frac{c}{2}\right)^2 = \frac{(\lambda_1 - \lambda_0)^2 + c^2}{4}, \tag{23}$$

where (23) describes the circumference having respectively center and radius given by

$$\left[\frac{\lambda_0 + \lambda_1 + 2}{2}, -\frac{c}{2}\right]^T \qquad \text{and} \qquad \frac{\sqrt{(\lambda_1 - \lambda_0)^2 + c^2}}{2}.$$

Now, taking $\lambda_0 = \lambda_1 = \lambda \geq 1$ and c as in the first part of (19), condition (13) is verified with the third inequality being actually an equality. Substituting these conditions into (23) we obtain a quadratic equation in λ that has always at least one solution for $\mathbf{p} \in \mathcal{P}_{\geq 1}([\rho, 0]^T)$. The explicit solutions for λ are exactly the ones shown by (18), first part. A similar argument can be applied for $\mathbf{p} \in \mathcal{P}_{<1}([\rho, 0]^T)$, giving the second part of (18) and (19). □

Remark 3.5. For $\lambda_0 = \lambda_1 = \lambda > 0$ the circumferences in (23) for c as in (19) describe all the circumferences contained in $\mathcal{P}_{\geq 1}([\rho, 0]^T) \cup \mathcal{P}_{<1}([\rho, 0]^T)$ which are tangent to the line $y = 0$ and to the border of $\mathcal{P}_{\geq 1}([\rho, 0]^T)$, if $\lambda \geq 1$, or to the border of $\mathcal{P}_{<1}([\rho, 0]^T)$, if $\lambda \in (0, 1)$.

Given $\mathbf{p}_{k-1}$ and $\mathbf{p}_k$, Corollary 3.3 can be used to locate the control point $\mathbf{p}_{k+1}$, for every class A special Bézier curve defined by a matrix characterized by Theorem 3.2. Indeed, since

$$\mathbf{p}_{k+1} - \mathbf{p}_{k-1} = \mathbf{M}^k\mathbf{v} + \mathbf{M}^{k-1}\mathbf{v} = \mathbf{M}(\mathbf{M}^{k-1}\mathbf{v}) + \mathbf{M}^{k-1}\mathbf{v} = \mathbf{M}(\mathbf{p}_k - \mathbf{p}_{k-1}) + (\mathbf{p}_k - \mathbf{p}_{k-1})$$

we can write

$$\mathbf{p}_{k+1} - \mathbf{p}_{k-1} \in \begin{cases} \mathcal{P}_{\geq 1}(\mathbf{p}_k - \mathbf{p}_{k-1}), & \text{if } \mathbf{M} \equiv \mathbf{M}_R \text{ satisfying (13)}, \\ \mathcal{P}_{<1}(\mathbf{p}_k - \mathbf{p}_{k-1}), & \text{if } \mathbf{M} \equiv \mathbf{M}_R \text{ satisfying (14)}. \end{cases} \tag{24}$$

In particular, (24) holds for $\mathbf{p}_0$, $\mathbf{p}_1$ and $\mathbf{p}_2$ which define the value of the curvature of the resulting Bézier curve at 0 via the well-known formula

$$\kappa(0) = \frac{n-1}{n} \frac{\left|\det\left[\mathbf{p}_1 - \mathbf{p}_0, \mathbf{p}_2 - \mathbf{p}_1\right]\right|}{\|\mathbf{p}_1 - \mathbf{p}_0\|^3} = \frac{n-1}{n} \frac{\left|\det\left[\mathbf{v}, \mathbf{M}\mathbf{v}\right]\right|}{\|\mathbf{v}\|^3},$$

where $n \in \mathbb{N}$ is the degree of the curve. Since we can translate and rotate a curve without affecting its curvature, we can always consider $\mathbf{p}_0 = \mathbf{0}$ and $\mathbf{p}_1 = [\rho, 0]^T$, $\rho > 0$, i.e., $\mathbf{v} = [\rho, 0]^T$. Then, for every choice of $\mathbf{p}_2 = [x_2, y_2]^T \in \mathcal{P}_{\geq 1}(\mathbf{v}) \cup \mathcal{P}_{<1}(\mathbf{v})$, we get

$$\kappa(0) \;=\; \frac{n-1}{n}\,\frac{|y_2|}{\rho^2}. \tag{25}$$

Corollary 3.3 can thus be used to construct class A special Bézier curves with prescribed initial control point, initial tangent and initial curvature value. Indeed, once we choose the degree n and the first three control points, all the geometric information about the resulting curve at 0 are fixed, and we can guarantee the class A property choosing $\mathbf{p}_2$ either in $\mathcal{P}_{\geq 1}(\mathbf{v})$ (for non-increasing curvature) or in $\mathcal{P}_{<1}(\mathbf{v})$ (for non-decreasing curvature). Equations (17), (18) and (19) then give us suitable choices of $\mathbf{M}$ to construct such class A special Bézier curves. Once the matrix $\mathbf{M}$ has been selected, the computation of the remaining control points is given by (2) and the curvature at 1 can be obtained as

$$\kappa(1) \;=\; \frac{n-1}{n}\,\frac{\left|\det\left[\mathbf{p}_{n-1}-\mathbf{p}_n, \mathbf{p}_{n-2}-\mathbf{p}_{n-1}\right]\right|}{\|\mathbf{p}_{n-1}-\mathbf{p}_n\|^3} \;=\; \frac{n-1}{n}\,\frac{\left|\det\left[\mathbf{M}^{n-1}\mathbf{v}, \mathbf{M}^{n-2}\mathbf{v}\right]\right|}{\|\mathbf{M}^{n-1}\mathbf{v}\|^3}. \tag{26}$$

Remark 3.6. Given $\mathbf{p}_0$, $\mathbf{p}_1$ and $\mathbf{p}_2$, there are actually infinitely many matrices $\mathbf{M}$ for which $\mathbf{p}_2 - \mathbf{p}_0 = \mathbf{M}(\mathbf{p}_1 - \mathbf{p}_0) + (\mathbf{p}_1 - \mathbf{p}_0)$ and Theorem 3.2 is satisfied. Here we highlighted the easiest construction which also coincides with the one farthest from the family of class A special Bézier curves described in Cao and Wang (2008), where, as already mentioned, the unique value of c allowed is 0. The choice (19) considers instead the largest admissible value of $|c|$ according to Theorem 3.2 and the case $c = 0$ only appears for the trivial case $\mathbf{M} = \mathbf{I}$. The resulting curves and associated curvatures are shown in Figure 4.

We conclude with an example showing the constructive approach of Corollay 3.3 for different choices of $\mathbf{p}_2 \in \mathcal{P}_{\geq 1}(\mathbf{v}) \cup \mathcal{P}_{<1}(\mathbf{v})$.

Example 3.2. Fixed $n = 5$, $\rho = 1$, $\mathbf{p}_0 = \mathbf{0}$ and $\mathbf{p}_1 = \mathbf{v} = [1, 0]^T$, we consider four different choices of $\mathbf{p}_2$: two of them in $\mathcal{P}_{<1}(\mathbf{v})$ (cases (a) and (b), Figure 3 and 4) and two of them in $\mathcal{P}_{\geq 1}(\mathbf{v})$ (cases (c) and (d), Figure 3 and 4). According to Corollary 3.3, for each choice of $\mathbf{p}_2$, we can choose two different pairs (λ, c) as in (18) and (19) leading to two matrices satisfying Theorem 3.2 and describing two different class A curves. Since the value of the curvature at 0 depends only on $\mathbf{p}_2$, see (25), for each case we have the same initial curvature but different values of the curvature at 1 given by (26). In particular,

(a) the choice $\mathbf{p}_2 = \begin{bmatrix}3/2, & 2/15\end{bmatrix}^T$ leads to two class A curves having respectively

- $(\lambda, c) = (0.5639, -0.1639)$, $\quad \mathbf{M} = \begin{bmatrix}0.5000 & -0.0306\\ 0.1333 & 0.6278\end{bmatrix}$, $\quad \kappa(0) = 0.1067$, $\quad \kappa(1) = 2.5445$,
- $(\lambda, c) = (0.4361, -0.1639)$, $\quad \mathbf{M} = \begin{bmatrix}0.5000 & -0.0306\\ 0.1333 & 0.3722\end{bmatrix}$, $\quad \kappa(0) = 0.1067$, $\quad \kappa(1) = 1.9301$;

(b) the choice $\mathbf{p}_2 = \begin{bmatrix}9/7, & -1/16\end{bmatrix}^T$ leads to two class A curves having respectively

- $(\lambda, c) = (0.3613, 0.1538)$, $\quad \mathbf{M} = \begin{bmatrix}0.2857 & 0.0913\\ -0.0625 & 0.4368\end{bmatrix}$, $\quad \kappa(0) = 0.05$, $\quad \kappa(1) = 62.5592$,
- $(\lambda, c) = (0.2273, 0.1171)$, $\quad \mathbf{M} = \begin{bmatrix}0.2857 & 0.0546\\ -0.0625 & 0.1689\end{bmatrix}$, $\quad \kappa(0) = 0.05$, $\quad \kappa(1) = 29.5270$;

(c) the choice $\mathbf{p}_2 = \begin{bmatrix}3, & 1/21\end{bmatrix}^T$ leads to two class A curves having respectively

- $(\lambda, c) = (2.1883, -0.7922)$, $\quad \mathbf{M} = \begin{bmatrix}2.0000 & -0.7446\\ 0.0476 & 2.3766\end{bmatrix}$, $\quad \kappa(0) = 0.0381$, $\quad \kappa(1) = 0.0012$,

- $(\lambda, c) = (1.8434, -0.5623)$, $\quad \mathbf{M} = \begin{bmatrix} 2.0000 & -0.5147 \\ 0.0476 & 1.6869 \end{bmatrix}$, $\quad \kappa(0) = 0.0381$, $\quad \kappa(1) = 4.0013e-04$;

(d) the choice $\mathbf{p}_2 = \begin{bmatrix} 4, & -7/6 \end{bmatrix}^T$ leads to two class A curves having respectively

- $(\lambda, c) = (3.9768, 1.9846)$, $\quad \mathbf{M} = \begin{bmatrix} 3.0000 & 0.8179 \\ -1.1667 & 4.9537 \end{bmatrix}$, $\quad \kappa(0) = 0.9333$, $\quad \kappa(1) = 1.4597e-04$,
- $(\lambda, c) = (2.8009, 1.2006)$, $\quad \mathbf{M} = \begin{bmatrix} 3.0000 & 0.0340 \\ -1.1667 & 2.6019 \end{bmatrix}$, $\quad \kappa(0) = 0.9333$, $\quad \kappa(1) = 2.0764e-04$.

Acknowledgements

This work has been accomplished within the "Research ITalian network on Approximation" (RITA) and the TAA-UMI group. The authors are members of the INdAM Research group GNCS, which has partially supported this work.

Appendix A. Proof of Theorem 3.2

For degree $n = 1$ the claimed result trivially follows. Consider then $n \geq 2$,

$$\mathbf{M} = \begin{bmatrix} \lambda_0 & c \\ 0 & \lambda_1 \end{bmatrix} \qquad \text{and} \qquad \mathbf{v} = \begin{bmatrix} v_0 \\ v_1 \end{bmatrix},$$

with $\lambda_0, \lambda_1 > 0$, $c \in \mathbb{R}$ and, without loss of generality, $v_0^2 + v_1^2 = 1$. We start observing two facts. First, we are able to compute the singular values of $\mathbf{M}$ exactly as

$$\begin{aligned} \sigma_\pm(\mathbf{M}) &= \sqrt{\frac{\lambda_0^2 + \lambda_1^2 + c^2 \ \pm \ \sqrt{(\lambda_0^2 + \lambda_1^2 + c^2)^2 - 4\lambda_0^2\lambda_1^2}}{2}} \\ &= \sqrt{\frac{\lambda_0^2 + \lambda_1^2 + c^2 \ \pm \ \sqrt{(\ (\lambda_0 + \lambda_1)^2 + c^2\ )\ (\ (\lambda_0 - \lambda_1)^2 + c^2\ )}}{2}}. \end{aligned} \tag{A.1}$$

Second, since

$$\mathbf{M}^{-1} = \begin{bmatrix} \dfrac{1}{\lambda_0} & -\dfrac{c}{\lambda_0\lambda_1} \\ 0 & \dfrac{1}{\lambda_1} \end{bmatrix} \tag{A.2}$$

describes the same curve as $\mathbf{M}$ but travelled backwards, we only need to study the case

$$\begin{bmatrix} \lambda_0 \\ \lambda_1 \end{bmatrix} \in H_{up} := \left\{ \begin{bmatrix} a \\ b \end{bmatrix} \in \mathbb{R}^2 \ : \ a > 0 \ \wedge \ b \geq 1 \right\}.$$

Doing so we will arrive to (13): (14) is then obtained by substituting λ_0, λ_1 and c with $1/\lambda_0$, $1/\lambda_1$ and $-c/(\lambda_0\lambda_1)$, respectively, as in (A.2). Indeed, the map

$$\begin{aligned} \mathcal{I}: \quad \mathbb{R}^2_+ &\longrightarrow \mathbb{R}^2_+ \\ \begin{bmatrix} \lambda_0 \\ \lambda_1 \end{bmatrix} &\longmapsto \begin{bmatrix} 1/\lambda_0 \\ 1/\lambda_1 \end{bmatrix} \end{aligned}$$

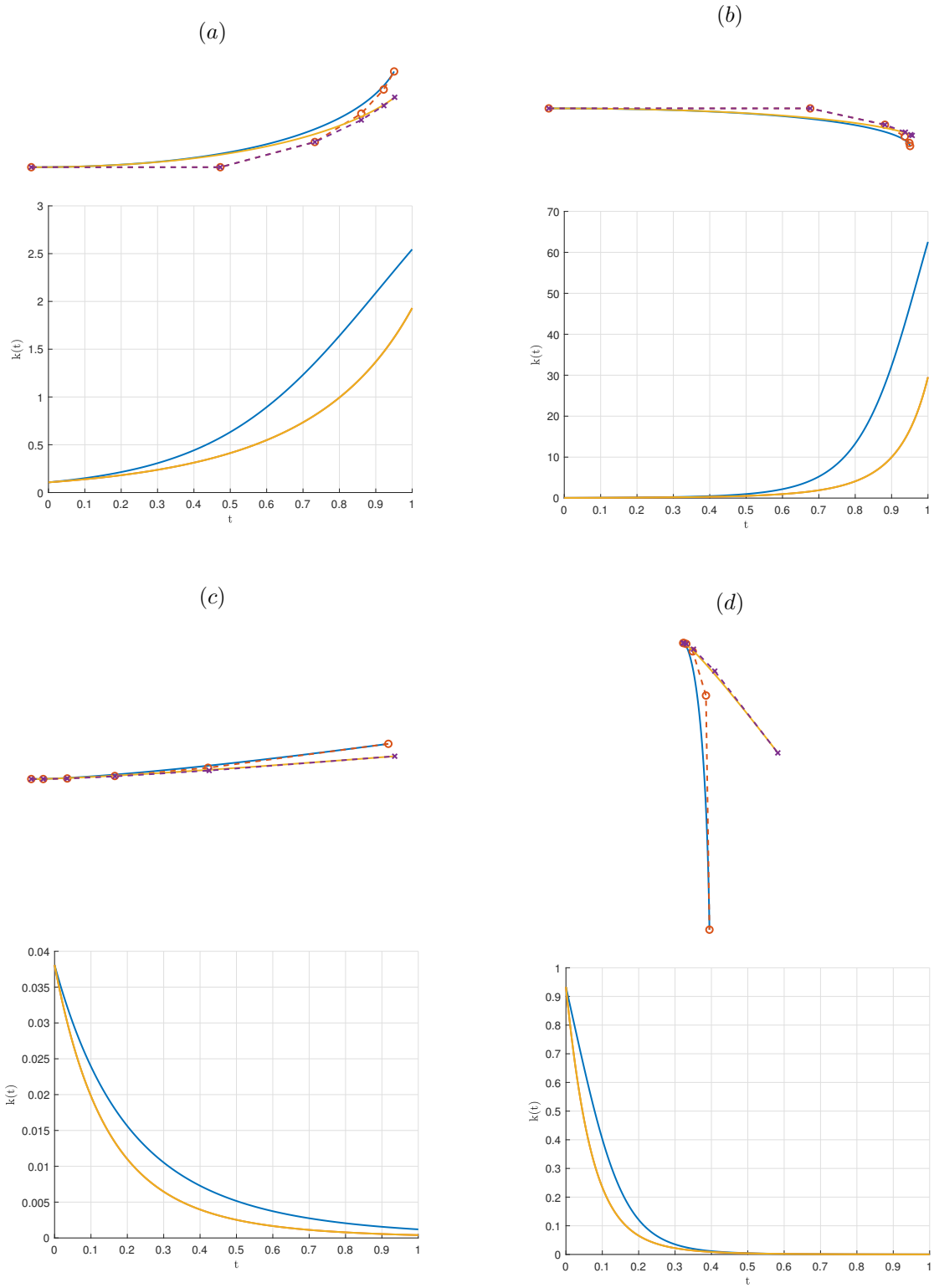

Figure 4: The class A special Bézier curves described in Example 3.2 and their associated curvature plots.

is such that $\mathcal{I}(H_{up}) = H_{down}$ where

$$H_{down} \;:=\; \left\{ \begin{bmatrix} a \\ b \end{bmatrix} \in \mathbb{R}^2 \;:\; a > 0 \;\wedge\; 0 < b \leq 1 \right\}$$

and $H_{up} \cup H_{down}$ is exactly $\mathbb{R}^2_+$.

Consider then $[\lambda_0, \lambda_1]^T \in H_{up}$. Plugging

$$\|\mathbf{M}\mathbf{v}\|^2 \;=\; (\lambda_0 v_0 + c v_1)^2 \;+\; \lambda_1^2 v_1^2 \qquad \text{and} \qquad \|(\mathbf{M} - \mathbf{I})\mathbf{v}\|^2 \;=\; [(\lambda_0 - 1)v_0 + c v_1]^2 \;+\; (\lambda_1 - 1)^2 v_1^2$$

in (8), it is easy to get

$$F(\mathbf{M}, \mathbf{v}) \;=\; 4\, v_1^2 \left((\lambda_0 - \lambda_1) v_0 \;+\; c v_1 \right)^2.$$

To characterize the curve with non-increasing curvature we need to ask $\kappa(0) \geq \kappa(1)$ which, due to Proposition 2.3, is equivalent to

$$4\, v_1^2 \left((\lambda_0 - \lambda_1) v_0 \;+\; c v_1 \right)^2 \;\geq\; \frac{\|\mathbf{M}^{n-2}\mathbf{v}\|^4}{\|\mathbf{M}^{n-1}\mathbf{v}\|^6}\, 4\, w_1^2 \left((\lambda_0 - \lambda_1) w_0 \;+\; c w_1 \right)^2$$

where

$$w_0 \;=\; \frac{\lambda_0^{n-2} v_0 \;+\; c \left(\displaystyle\sum_{k=0}^{n-3} \lambda_0^k\, \lambda_1^{n-3-k} \right) v_1}{\|\mathbf{M}^{n-2}\mathbf{v}\|} \qquad \text{and} \qquad w_1 \;=\; \frac{\lambda_1^{n-2} v_1}{\|\mathbf{M}^{n-2}\mathbf{v}\|}.$$

Thus, we need

$$v_1^2 \left((\lambda_0 - \lambda_1) v_0 \;+\; c v_1 \right)^2 \;\geq\; \frac{(\lambda_0 \lambda_1)^{2n-4}}{\|\mathbf{M}^{n-1}\mathbf{v}\|^6} v_1^2 \left((\lambda_0 - \lambda_1) v_0 \;+\; c v_1 \right)^2$$

to hold for every $n \geq 2$ and every unit vector $\mathbf{v}$. This requires, for every $n \geq 2$,

$$1 \;\geq\; \frac{(\lambda_0 \lambda_1)^{2n-4}}{\sigma_-(\mathbf{M})^{6n-6}} \quad \Longleftrightarrow \quad \sigma_-(\mathbf{M})^2 \;\geq\; (\lambda_0 \lambda_1)^{\frac{2n-4}{3n-3}}$$

which means $\sigma_-(\mathbf{M})^2 \;\geq\; \max\{1, (\lambda_0 \lambda_1)^{2/3}\}$. The condition $\sigma_-(\mathbf{M})^2 \geq 1$, thanks to (A.1), is equivalent to

$$2 - \lambda_0^2 - \lambda_1^2 \;\leq\; c^2 \;\leq\; (\lambda_0^2 - 1)(\lambda_1^2 - 1) \tag{A.3}$$

which describes a non-empty set if and only if $\min\{\lambda_0, \lambda_1\} \geq 1$, since we are considering $[\lambda_0, \lambda_1]^T \in H_{up}$. On the other hand, the condition $\sigma_-(\mathbf{M})^2 \geq (\lambda_0 \lambda_1)^{2/3}$ coincides with

$$\begin{cases} c^2 \;\geq\; 2(\lambda_0 \lambda_1)^{2/3} - \lambda_0^2 - \lambda_1^2 \;=:\; \widetilde{L}(\lambda_0, \lambda_1) \\[2ex] c^2 \;\leq\; (\lambda_0 \lambda_1)^{4/3} \;+\; (\lambda_0 \lambda_1)^{2/3} \;-\; \lambda_0^2 \;-\; \lambda_1^2 \;=:\; \widetilde{U}(\lambda_0, \lambda_1) \end{cases} \tag{A.4}$$

which is a stronger condition than (A.3) for $\min\{\lambda_0, \lambda_1\} \geq 1$ and add the requirement

$$\sqrt{\lambda_0} \;\leq\; \lambda_1 \;\leq\; \lambda_0^2. \tag{A.5}$$

At this point, we proceed subdividing the curve at $r \in (0, 1)$. Thus, due to (12), we need to deal with the following matrices

$$\mathbf{M}_{[0,r]} \;=\; \begin{bmatrix} 1 + r(\lambda_0 - 1) & c r \\ 0 & 1 + r(\lambda_1 - 1) \end{bmatrix},$$

$$\mathbf{M}_{[r,1]} \;=\; \begin{bmatrix} \dfrac{\lambda_0}{1 + r(\lambda_0 - 1)} & \dfrac{c(1 - r)}{(\,1 + r(\lambda_0 - 1)\,)\,(\,1 + r(\lambda_1 - 1)\,)} \\[2ex] 0 & \dfrac{\lambda_1}{1 + r(\lambda_1 - 1)} \end{bmatrix}. \tag{A.6}$$

Then $\mathbf{M}$ always leads to class A curves if and only if, for every $r \in (0,1)$, the matrices in (A.6) satisfy (A.4) and (A.5), where λ_0, λ_1 and c are replaced with the corresponding eigenvalues and off-diagonal entry, respectively. First, to guarantee the inheritance of (A.5), we must find Ω_{up} as the largest subset of $\{\, [\lambda_0, \lambda_1]^T \in \mathbb{R}^2 \;:\; \sqrt{\lambda_0} \le \lambda_1 \le \lambda_0^2,\ \lambda_0 \ge 1 \,\}$ for which

$$\begin{bmatrix} \lambda_0 \\ \lambda_1 \end{bmatrix} \in \Omega_{up} \quad \Longrightarrow \quad \begin{cases} [\, 1 + r(\lambda_0 - 1),\ 1 + r(\lambda_1 - 1) \,]^T \in \Omega_{up}, \\ \left[\dfrac{\lambda_0}{1 + r(\lambda_0 - 1)},\ \dfrac{\lambda_1}{1 + r(\lambda_1 - 1)} \right]^T \in \Omega_{up}, \end{cases} \qquad \forall r \in (0,1).$$

Since $\{\, [\, 1 + r(\lambda_0 - 1),\ 1 + r(\lambda_1 - 1) \,]^T \,\}_{r \in (0,1)}$, corresponds to the segment connecting $[\lambda_0, \lambda_1]^T$ to $[1,1]^T$, it is easy to check that Ω_{up} must be included in the cone delimited by the tangents at $[1,1]^T$ of the two functions $\lambda_1 = \sqrt{\lambda_0}$ and $\lambda_1 = \lambda_0^2$ (see Figure 1, left), i.e.

$$\Omega_{up} \;\subseteq\; \left\{ \begin{bmatrix} \lambda_0 \\ \lambda_1 \end{bmatrix} \in \mathbb{R}^2 \;:\; \frac{\lambda_0 + 1}{2} \le \lambda_1 \le 2\lambda_0 - 1,\ \lambda_0 \;\ge\; 1 \right\}.$$

More precisely,

$$\Omega_{up} \;=\; \left\{ \begin{bmatrix} \lambda_0 \\ \lambda_1 \end{bmatrix} \in \mathbb{R}^2 \;:\; \frac{\lambda_0 + 1}{2} \le \lambda_1 \le 2\lambda_0 - 1,\ \lambda_0 \;\ge\; 1 \right\}. \tag{A.7}$$

Indeed,

$$\frac{1}{2}\left(\frac{\lambda_0}{1 + r(\lambda_0 - 1)} \;+\; 1 \right) \;\le\; \frac{\lambda_1}{1 + r(\lambda_1 - 1)} \;\le\; 2\,\frac{\lambda_0}{1 + r(\lambda_0 - 1)} \;-\; 1, \quad \forall r \in (0,1)$$

$$\Updownarrow$$

$$\frac{1}{2}\left(\frac{\lambda_0}{1 + r(\lambda_0 - 1)} \;+\; 1 \right) \;\le\; \frac{\lambda_1}{1 + r(\lambda_1 - 1)}, \quad \forall r \in (0,1)$$

$$\Updownarrow$$

$$P(r) \;:=\; r^2(\lambda_0 - 1)(\lambda_1 - 1) \;+\; r(3\lambda_1 - \lambda_0\lambda_1 - 2) \;+\; \lambda_0 - 2\lambda_1 + 1 \;\le\; 0, \quad \forall r \in (0,1),$$

where, since by (A.7) $\min\{\lambda_0, \lambda_1\} \ge 1$ for $[\lambda_0, \lambda_1]^T \in \Omega_{up}$, the parabola $P(r)$ opens upwards with $P(0) \le 0$ and $P(1) = 0$. Analogously,

$$\frac{\lambda_1}{1 + r(\lambda_1 - 1)} \;\le\; 2\,\frac{\lambda_0}{1 + r(\lambda_0 - 1)} \;-\; 1, \quad \forall r \in (0,1)$$

$$\Updownarrow$$

$$r^2(\lambda_0 - 1)(\lambda_1 - 1) \;+\; r(3\lambda_0 - \lambda_0\lambda_1 - 2) \;+\; \lambda_1 - 2\lambda_0 + 1 \;\le\; 0, \quad \forall r \in (0,1).$$

Now, defined,

$$L_1(\lambda_0, \lambda_1, r) \;:=\; \widetilde{L}\,(\, 1 + r(\lambda_0 - 1),\ 1 + r(\lambda_1 - 1)\,), \quad L_2(\lambda_0, \lambda_1, r) \;:=\; \widetilde{L}\left(\frac{\lambda_0}{1 + r(\lambda_0 - 1)}, \frac{\lambda_1}{1 + r(\lambda_1 - 1)} \right),$$

$$U_1(\lambda_0, \lambda_1, r) \;:=\; \widetilde{U}\,(\, 1 + r(\lambda_0 - 1),\ 1 + r(\lambda_1 - 1)\,), \quad U_2(\lambda_0, \lambda_1, r) \;:=\; \widetilde{U}\left(\frac{\lambda_0}{1 + r(\lambda_0 - 1)}, \frac{\lambda_1}{1 + r(\lambda_1 - 1)} \right),$$

the fact that the matrices in (A.6) inherit condition (A.4) from $\mathbf{M}$ is equivalent to

$$\left\{\begin{array}{l} c^2 \;\geq\; \max\left\{ \sup\limits_{r\in(0,1)} \dfrac{L_1(\lambda_0,\lambda_1,r)}{r^2},\; \sup\limits_{r\in(0,1)} \dfrac{(\,1+r(\lambda_0-1)\,)^2\,(\,1+r(\lambda_1-1)\,)^2}{(1-r)^2}\, L_2(\lambda_0,\lambda_1,r) \right\}, \\[2ex] c^2 \;\leq\; \min\left\{ \inf\limits_{r\in(0,1)} \dfrac{U_1(\lambda_0,\lambda_1,r)}{r^2},\; \inf\limits_{r\in(0,1)} \dfrac{(\,1+r(\lambda_0-1)\,)^2\,(\,1+r(\lambda_1-1)\,)^2}{(1-r)^2}\, U_2(\lambda_0,\lambda_1,r) \right\}. \end{array}\right. \tag{A.8}$$

For the lower bound, we have that $\widetilde{L}(\lambda_0,\lambda_1) \leq 0$, since $\min\{\lambda_0,\lambda_1\} \geq 1$ and

$$\widetilde{L}(\lambda_0,\lambda_1) \;\leq\; 0 \quad\Longleftrightarrow\quad 2(\lambda_0\lambda_1)^{2/3} \;\leq\; \lambda_0^2+\lambda_1^2.$$

Moreover, for every $r \in (0,1)$,

$$\min\{\,1+r(\lambda_0-1),\; 1+r(\lambda_1-1)\,\} \;\geq\; 1 \quad\text{and}\quad \min\left\{\frac{\lambda_0}{1+r(\lambda_0-1)},\; \frac{\lambda_1}{1+r(\lambda_1-1)}\right\} \;\geq\; 1.$$

and so, for every fixed $[\lambda_0,\lambda_1]^T \in \Omega_{up}$,

$$\max\{\,L_1(\lambda_0,\lambda_1,r),\; L_2(\lambda_0,\lambda_1,r)\,\} \;\leq\; 0, \quad \forall r \in (0,1).$$

This implies that the lower bound for c^2 in (A.8) is always satisfied.

For the upper bound in (A.8), we study the two infimum separately. Since the case $\lambda_0 = \lambda_1 = 1$ admits only $c = 0$, we can consider $[\lambda_0,\lambda_1]^T \in \Omega_{up} \setminus \{[1,1]^T\}$. Starting from $U_1(\lambda_0,\lambda_1,r)/r^2$, we use the substitutions

$$\left\{\begin{array}{lllllllll} x & = & (1+r(\lambda_0-1))^{1/3} & \longrightarrow & x^3 & = & 1+r(\lambda_0-1) & \longrightarrow & r \;=\; \dfrac{x^3-1}{\lambda_0-1} \\[2ex] y & = & (1+r(\lambda_1-1))^{1/3} & \longrightarrow & y^3 & = & 1+r(\lambda_1-1) & \longrightarrow & r \;=\; \dfrac{y^3-1}{\lambda_1-1} \end{array}\right.$$

and obtain

$$\begin{aligned} \frac{U_1(\lambda_0,\lambda_1,r)}{r^2} \;&=\; \frac{x^4y^4 \;+\; x^2y^2 \;-\; x^6 \;-\; y^6}{r^2} \\ &=\; \frac{(x^2-1)\,(y^2-1)\,(x^2y^2+x^2+y^2+2)}{r^2} \;-\; \frac{(x^2-1)^2\,(x^2+1)}{r^2} \;-\; \frac{(y^2-1)^2\,(y^2+1)}{r^2} \\ &=\; (\lambda_0-1)\,(\lambda_1-1)\,\frac{(x^2-1)\,(y^2-1)\,(x^2y^2+x^2+y^2+2)}{(x^3-1)\,(y^3-1)} \;+ \\ &\qquad -\,(\lambda_0-1)^2\,\frac{(x^2-1)^2\,(x^2+1)}{(x^3-1)^2} \;-\; (\lambda_1-1)^2\,\frac{(y^2-1)^2\,(y^2+1)}{(y^3-1)^2} \\ &=\; (\lambda_0-1)\,(\lambda_1-1)\,\frac{(x+1)\,(y+1)\,(x^2y^2+x^2+y^2+2)}{(x^2+x+1)\,(y^2+y+1)} \;+ \\ &\qquad -\,(\lambda_0-1)^2\,\frac{(x+1)^2\,(x^2+1)}{(x^2+x+1)^2} \;-\; (\lambda_1-1)^2\,\frac{(y+1)^2\,(y^2+1)}{(y^2+y+1)^2} \\ &=\; \Big(\,(\lambda_0-1)\,f(x) \;+\; (\lambda_1-1)\,g(y)\,\Big)\,\Big(\,(\lambda_0-1)\,g(x) \;+\; (\lambda_1-1)\,f(y)\,\Big), \end{aligned}$$

where

$$f(x) \;:=\; \frac{(x+1)\,(x^2+1)}{x^2+x+1} \quad \text{and} \quad g(x) \;:=\; -\,\frac{x+1}{x^2+x+1}. \tag{A.9}$$

Since f and g are both monotonically increasing when their argument is non-negative and $[x,y]^T \in \left(1, \lambda_0^{1/3}\right) \times \left(1, \lambda_1^{1/3}\right)$, then

$$\left\{ \begin{array}{l} (\lambda_0-1)\,f(x) \;+\; (\lambda_1-1)\,g(y) \;\geq\; (\lambda_0-1)\,f(1) \;+\; (\lambda_1-1)\,g(1) \;=\; \dfrac{2}{3}\,(2\lambda_0-\lambda_1-1), \\[2ex] (\lambda_0-1)\,g(x) \;+\; (\lambda_1-1)\,f(y) \;\geq\; (\lambda_0-1)\,g(1) \;+\; (\lambda_1-1)\,f(1) \;=\; \dfrac{2}{3}\,(2\lambda_1-\lambda_0-1), \end{array} \right. \tag{A.10}$$

where the right-hand sides of (A.10) are both non-negative for $[\lambda_0,\lambda_1]^T \in \Omega_{up}$. Thus, for every $r \in (0,1)$

$$\frac{U_1(\lambda_0,\lambda_1,r)}{r^2} \;\geq\; \frac{4}{9}\,(2\lambda_0-\lambda_1-1)\,(2\lambda_1-\lambda_0-1).$$

Moreover, since $[x,y]^T \to [1,1]^T$ for $r \to 0^+$, we have

$$\inf_{r\in(0,1)} \frac{U_1(\lambda_0,\lambda_1,r)}{r^2} \;=\; \frac{4}{9}\,(2\lambda_0-\lambda_1-1)\,(2\lambda_1-\lambda_0-1).$$

In a similar way, we use the substitutions

$$\left\{ \begin{array}{lllllllll} x & = & \left(\dfrac{1+r(\lambda_0-1)}{\lambda_0}\right)^{1/3} & \longrightarrow & r \;=\; \dfrac{\lambda_0 x^3-1}{\lambda_0-1} & \longrightarrow & 1-r \;=\; \dfrac{\lambda_0(1-x^3)}{\lambda_0-1} \\[2ex] y & = & \left(\dfrac{1+r(\lambda_1-1)}{\lambda_1}\right)^{1/3} & \longrightarrow & r \;=\; \dfrac{\lambda_1 y^3-1}{\lambda_1-1} & \longrightarrow & 1-r \;=\; \dfrac{\lambda_1(1-y^3)}{\lambda_1-1} \end{array} \right.$$

and get

$$\begin{aligned} &\frac{(\,1+r(\lambda_0-1)\,)^2\,(\,1+r(\lambda_1-1)\,)^2}{(1-r)^2}\,U_2(\lambda_0,\lambda_1,r) \\ &\quad= \lambda_0^2\,\lambda_1^2\,\frac{x^4y^4 \;+\; x^2y^2 \;-\; x^6 \;-\; y^6}{(1-r)^2} \\ &\quad= \lambda_0^2\,\lambda_1^2\left(\frac{(x^2-1)\,(y^2-1)\,(x^2y^2+x^2+y^2+2)}{(1-r)^2} \;-\; \frac{(x^2-1)^2\,(x^2+1)}{(1-r)^2} \;-\; \frac{(y^2-1)^2\,(y^2+1)}{(1-r)^2}\right) \\ &\quad= \lambda_0^2\,\lambda_1^2\left(\frac{(\lambda_0-1)\,(\lambda_1-1)\,(x^2-1)\,(y^2-1)\,(x^2y^2+x^2+y^2+2)}{\lambda_0\,\lambda_1\,(1-x^3)\,(1-y^3)}\right. \\ &\qquad\qquad \left. -\,\frac{(\lambda_0-1)^2\,(x^2-1)^2\,(x^2+1)}{\lambda_0^2\,(1-x^3)^2} \;-\; \frac{(\lambda_1-1)^2\,(y^2-1)^2\,(y^2+1)}{\lambda_1^2\,(1-y^3)^2}\right) \\ &\quad= \lambda_0^2\,\lambda_1^2\left(\frac{(\lambda_0-1)\,(\lambda_1-1)}{\lambda_0\,\lambda_1}\,\frac{(x+1)\,(y+1)\,(x^2y^2+x^2+y^2+2)}{(x^2+x+1)\,(y^2+y+1)}\right. \\ &\qquad\qquad \left. -\,\frac{(\lambda_0-1)^2}{\lambda_0^2}\,\frac{(x+1)^2\,(x^2+1)}{(x^2+x+1)^2} \;-\; \frac{(\lambda_1-1)^2}{\lambda_1^2}\,\frac{(y+1)^2\,(y^2+1)}{(y^2+y+1)^2}\right) \\ &\quad= \Big(\,\lambda_1(\lambda_0-1)f(x) \;+\; \lambda_0(\lambda_1-1)g(y)\,\Big)\,\Big(\,\lambda_1(\lambda_0-1)\,g(x) \;+\; \lambda_0(\lambda_1-1)f(y)\,\Big), \end{aligned}$$

where f and g are as in (A.9). Again, since f and g are both monotonically increasing when their argument is greater than 0 and $[x,y]^T \in \left(\lambda_0^{-1/3},1\right) \times \left(\lambda_1^{-1/3},1\right)$, then

$$\begin{cases} \lambda_1(\lambda_0-1)f(x)+\lambda_0(\lambda_1-1)g(y) \geq \lambda_1(\lambda_0-1)f(\lambda_0^{-1/3})+\lambda_0(\lambda_1-1)g(\lambda_1^{-1/3}) = (\lambda_0^{4/3}-\lambda_1^{2/3}), \\ \lambda_1(\lambda_0-1)g(x)+\lambda_0(\lambda_1-1)f(y) \geq \lambda_1(\lambda_0-1)g(\lambda_0^{-1/3})+\lambda_0(\lambda_1-1)f(\lambda_1^{-1/3}) = (\lambda_1^{4/3}-\lambda_0^{2/3}), \end{cases} \tag{A.11}$$

where the right-hand sides of (A.11) are both non-negative for $[\lambda_0,\lambda_1]^T \in \Omega_{up}$. Thus, for every $r \in (0,1)$,

$$\frac{(\,1+r(\lambda_0-1)\,)^2\,(\,1+r(\lambda_1-1)\,)^2}{(1-r)^2}\,U_2(\lambda_0,\lambda_1,r) \quad \geq \quad (\lambda_0^{4/3}-\lambda_1^{2/3})\,(\lambda_1^{4/3}-\lambda_0^{2/3}).$$

Moreover, since $[x,y]^T \to [\lambda_0^{-1/3},\lambda_1^{-1/3}]^T$ for $r \to 0^+$, we have

$$\inf_{r\in(0,1)} \frac{(\,1+r(\lambda_0-1)\,)^2\,(\,1+r(\lambda_1-1)\,)^2}{(1-r)^2}\,U_2(\lambda_0,\lambda_1,r) \;=\; (\lambda_0^{4/3}-\lambda_1^{2/3})\,(\lambda_1^{4/3}-\lambda_0^{2/3}).$$

To conclude the proof we only have to observe that, for every $[\lambda_0,\lambda_1]^T \in \Omega_{up}$,

$$\frac{4}{9}\,(2\lambda_0-\lambda_1-1)\,(2\lambda_1-\lambda_0-1) \;\leq\; (\lambda_0^{4/3}-\lambda_1^{2/3})\,(\lambda_1^{4/3}-\lambda_0^{2/3}).$$

□

References

Cantón, A., Fernández-Jambrina, L., Vázquez-Gallo, M.J., 2021. Curvature of planar aesthetic curves. J. Comput. Appl. Math. 381, 113042, 19. URL: https://doi.org/10.1016/j.cam.2020.113042, doi:10.1016/j.cam.2020.113042.

Cao, J., Wang, G., 2008. A note on: "Class A Bézier curves" [Comput. Aided Geom. Design **23** (2006), no. 7, 573–581; mr2250471] by G. Farin. Comput. Aided Geom. Design 25, 523–528. URL: https://doi.org/10.1016/j.cagd.2007.10.001, doi:10.1016/j.cagd.2007.10.001.

Farin, G., 2006. Class A Bézier curves. Comput. Aided Geom. Design 23, 573–581. URL: https://doi.org/10.1016/j.cagd.2006.03.004, doi:10.1016/j.cagd.2006.03.004.

Mineur, Y., Lichah, T., Castelain, J.M., Giaume, H., 1998. A shape controlled fitting method for Bézier curves. Comput. Aided Geom. Design 15, 879–891. URL: https://doi.org/10.1016/S0167-8396(98)00025-9, doi:10.1016/S0167-8396(98)00025-9.

Sapidis, N.S., Frey, W.H., 1992. Controlling the curvature of a quadratic Bézier curve. Comput. Aided Geom. Design 9, 85–91. URL: https://doi.org/10.1016/0167-8396(92)90008-D, doi:10.1016/0167-8396(92)90008-D.

Tong, W., Chen, M., 2021. A sufficient condition for 3d typical curves. Computer Aided Geometric Design 87, 101991. URL: https://www.sciencedirect.com/science/article/pii/S0167839621000364, doi:https://doi.org/10.1016/j.cagd.2021.101991.

Wang, A., Zhao, G., 2018. Counter examples of "Class A Bézier curves". Comput. Aided Geom. Design 61, 6–8. URL: https://doi.org/10.1016/j.cagd.2018.02.001, doi:10.1016/j.cagd.2018.02.001.

Wang, A., Zhao, G., Hou, F., 2019. Constructing Bézier curves with monotone curvature. J. Comput. Appl. Math. 355, 1–10. URL: https://doi.org/10.1016/j.cam.2019.01.004, doi:10.1016/j.cam.2019.01.004.

Wang, Y., Zhao, B., Zhang, L., Xu, J., Wang, K., Wang, S., 2004. Designing fair curves using monotone curvature pieces. Comput. Aided Geom. Design 21, 515–527. URL: https://doi.org/10.1016/j.cagd.2004.04.001, doi:10.1016/j.cagd.2004.04.001.

Yoshida, N., Hiraiwa, T., Saito, T., 2008. Interactive control of planar class A Bézier curves using logarithmic curvature graphs. Computer-Aided Design and Applications 5, 121–130.